

# Effective equilibrium picture in $xy$ -model with exponentially correlated noise

Matteo Paoluzzi<sup>1,\*</sup>, Umberto Marini Bettolo Marconi<sup>2</sup>, and Claudio Maggi<sup>3</sup>

<sup>1</sup> *Department of Physics and Syracuse Soft Matter Program, Syracuse University, Syracuse NY 13244, USA*

<sup>2</sup> *Scuola di Scienze e Tecnologie, Università di Camerino,*

*Via Madonna delle Carceri, 62032, Camerino, INFN Perugia, Italy*

<sup>3</sup> *NANOTEC-CNR, Institute of Nanotechnology,*

*Soft and Living Matter Laboratory, Piazzale A. Moro 2, I-00185, Roma, Italy*

We study the effect of exponentially correlated noise on  $xy$ -model in the limit of small correlation time discussing the order-disorder transition in mean field and the topological transition in two dimensions. We map the steady states of the non-equilibrium dynamics into an effective equilibrium theory. In mean-field, the critical temperature increases with the noise correlation time  $\tau$  indicating that memory effects promote ordering. This finding is confirmed by numerical simulations. The topological transition temperature in two dimensions remains untouched. However, finite size effects induce a crossover in the vortices proliferation that is confirmed by numerical simulations.

## I. INTRODUCTION

The classical  $xy$ -model undergoes a phase transition that is second order in  $d > 2$  spatial dimensions and infinite order in  $d = 2$  [1, 2]. Since  $xy$ -model is described by a vectorial order parameter invariant under  $O(2)$  orthogonal symmetry group, the existence of a second order phase transition in  $d$  spatial dimensions is governed by Mermin-Wagner theorem that fixes the lower critical dimension at  $d = 2$  [3–5]. However, in two dimensions, topological defects produce collective configurations like vortices that cause a novel type of phase transition related to the vortex/anti-vortex pair unbinding [6–8], i. e., the so-called Berezinskii-Kosterlitz-Thouless transition (BKT).

In this paper, we investigate the properties of  $xy$ -model driven out-of-equilibrium through exponentially correlated noise. The control parameters of the dynamics are the correlation time of the noise  $\tau$  and the strength of the noise  $T$ . When  $\tau = 0$ , the model reduces to the equilibrium  $xy$ -model at temperature  $T$ . By considering Unified Colored Noise Approximation (UCNA) [9, 10] in the small  $\tau$  limit, we write an effective equilibrium theory that is exact in the small  $\tau$  limit. In the effective equilibrium picture,  $\tau$  becomes an external thermodynamic parameter that can be tuned to bring the system to the transition point.

We will start by discussing the model in mean-field approximation corresponding to  $d = \infty$ . To do so, we consider a fully-connected lattice [11]. In the small  $\tau$  limit, we can compute analytically the partition function obtaining a vectorial  $O(2)$  field-theory where the Landau parameters depend on both, temperature and  $\tau$ . According to that finding, the mean-field model for small  $\tau$  undergoes a second order phase transition at a  $\tau$  dependent temperature. We show that, as well the scalar field theories [12], exponentially correlated noise promotes order in the sense that the resulting mean-field critical tem-

perature  $T_{mf}(\tau)$  is an increasing function of  $\tau$ , i. e., by increasing  $\tau$  the critical temperature increases too.

After that, we will address the problem in  $d = 2$ , where for  $\tau = 0$  the second order phase transition is replaced by BTK transition at temperature  $T_{BKT}$ . In that case, the effective equilibrium picture is obtained considering the continuum limit of  $xy$ -model, i. e., in the spin-wave approximation. From the computation of the spatial correlation function, we show that no long-range order can be obtained at small but finite  $\tau$ . The impact of  $\tau$  on BKT will be investigated considering the single vortex energy cost. Even though the effect of correlated noise becomes negligible in the thermodynamic limit, we find a linear shift at higher temperature  $T_{BKT}$  that scales logarithmically in the system size.

In Active Matter [13–17], recent works pointed out the importance of memory effects on the angular dynamics of Vicsek like models [18, 19]. However, in the presence of memory effects, it is not possible to perform the usual coarse graining procedure to obtain hydrodynamic equations [14, 18]. In the model we are going to consider, since the calculation is performed on a lattice, density fluctuations are not taken into account. However, the effective equilibrium picture could be extended to off-lattice model.

We also perform numerical simulations to check the validity of the approximated solution. We compare the predictions given by the approximated theory with numerical simulations for both cases, mean-field and two dimensions. In particular, the theoretical expression for the critical temperature in mean-field is in good agreement with numerical simulations. In two dimensions, we recover a linear shift in  $\tau$ , in agreement with the prediction of the theory.

## II. THE MODEL

We consider the dynamics of a two dimensional  $xy$ -model driven by exponentially correlated noise. The system is composed by  $N$  compasses  $\mathbf{s}_i = (\cos \theta_i, \sin \theta_i)$ , with  $i = 1, \dots, N$ , arranged on a two dimensional square

\* mpaoluzz@syr.edu

lattice. The model can be introduced formally by considering the following equation of motion for the angular degree of freedom  $\theta_i$

$$\dot{\theta}_i = -\frac{\partial H_{xy}}{\partial \theta_i} + \zeta_i. \quad (1)$$

The Hamiltonian is

$$H_{xy}[\theta] = -\frac{1}{2} \sum_{i,j} J_{ij} \cos(\theta_i - \theta_j) \quad (2)$$

where  $J_{ij}$  is the adjacency matrix. In mean-field,  $J_{ij} = J/N$ ,  $\forall i, j = 1, \dots, N$ , i. e., fully-connected lattice. In  $d$  dimensions,  $J_{ij} = J$  is different from zero only for nearest neighbors sites. We consider ferromagnetic coupling  $J > 0$ . The noise term  $\zeta_i$  is colored and Gaussian

$$\begin{aligned} \langle \zeta_i(t) \rangle &= 0 \\ \langle \zeta_i(t) \zeta_j(s) \rangle &= \frac{2T}{\tau} \delta_{ij} e^{-\frac{|t-s|}{\tau}} \end{aligned} \quad (3)$$

To start our analytical computation we rewrite (1) using an auxiliary variable  $\psi_i$  for each angular degree of freedom  $\theta_i$ . To ensure an exponentially correlated dynamics for  $\theta_i$ ,  $\psi_i$  undergoes an Ornstein-Uhlenbeck process. We can recast the original equations of motion (1) as follows

$$\begin{aligned} \dot{\theta}_i &= -\frac{\partial H_{xy}}{\partial \theta_i} + \psi_i, \\ \tau \dot{\psi}_i &= -\psi_i + \sqrt{T} \eta_i. \end{aligned} \quad (4)$$

Now the noise term  $\eta_i$  is white and Gaussian, i. e.,  $\langle \eta_i \rangle = 0$  and  $\langle \eta_i(t) \eta_j(s) \rangle = 2\delta_{ij} \delta(t-s)$ .  $T$  tunes the strength of the noise,  $\tau$  is the persistence time. When  $\tau = 0$ , our model reduces to the equilibrium  $xy$ -model at temperature  $T$ . In the opposite limit, i. e.,  $\tau \rightarrow \infty$  and  $T$  finite,  $\psi_i$  is a random and quenched variable and we recover the Kuramoto model [20]. It is worth noting that Eqs. (4) are the on-lattice version of the angular dynamics for self-propelled particles considered in [18].

Now we will write an equilibrium-like description of the steady state resulting from the non-equilibrium dynamics (4). To do so, we employ the Unified Colored Noise approximation (UCNA) [9, 21] to the many-body problem [10, 22–24]. We start with performing the time derivative of the first equation in (4). Adopting the dot notation for the time derivative and using the Einstein summation convention, one has [10]

$$\begin{aligned} \tau \ddot{\theta}_i &= -M_{ij} \dot{\theta}_j - \frac{\partial H_{xy}}{\partial \theta_i} + \sqrt{T} \eta_i \\ M_{ij} &\equiv \delta_{ij} + \tau \frac{\partial^2 H_{xy}}{\partial \theta_i \partial \theta_j}, \end{aligned} \quad (5)$$

According to (5), we have rewritten the original set of two first order stochastic differential equations into a second-order stochastic differential equation where  $\tau$  plays the role of inertia and  $M_{ij}$  is the friction. In UCNA one

consider the overdamped limit of (5), to do so let us introduce  $\tilde{M}_{ij} \equiv \tau^{1/2} M_{ij}$  and the rescaled time  $z = \tau^{-1/2} t$ . We can then write

$$\ddot{\theta}_i = -\tilde{M}_{ij} \dot{\theta}_j - \frac{\partial H_{xy}}{\partial \theta_i} + \tilde{\eta}_i \quad (6)$$

where for the noise term  $\tilde{\eta}$  one has  $\langle \tilde{\eta}_i \rangle = 0$  and  $\langle \tilde{\eta}_i(z) \tilde{\eta}_j(z') \rangle = 2T\tau^{-1/2} \delta_{ij} \delta(z-z')$ . The overdamped limit holds in the large and positive friction limit  $\tilde{M}_{ij} \gg 1$ . Since  $\tilde{M}_{ij} = \delta_{ij} \tau^{-1/2} + \tau^{1/2} \frac{\partial^2 H_{xy}}{\partial \theta_i \partial \theta_j}$ , in the region of the configuration space where the system is locally stable, i. e., where potential energy hypersurface has all positive curvatures, the large friction limit is realized in both situations  $\tau \rightarrow 0$  and  $\tau \rightarrow \infty$  [9, 21]. In the large friction limit we can write

$$\begin{aligned} \dot{\theta}_i &= -\frac{1}{2} F_i[\theta] + D_{ij}[\theta] \eta_j \\ F_i[\theta] &\equiv -2M_{ij}^{-1} \frac{\partial H_{xy}}{\partial \theta_i} \\ D_{ij}[\theta] &\equiv \sqrt{T} M_{ij}^{-1}. \end{aligned} \quad (7)$$

The corresponding Fokker-Planck equation for the probability distribution function  $P[\theta, t]$  reads

$$\partial_t P[\theta, t] = \frac{1}{2} \frac{\partial}{\partial \theta_i} \left\{ 2D_{ij} \frac{\partial}{\partial \theta_l} [D_{lj} P] + F_i P \right\}. \quad (8)$$

To compute the steady state distribution  $P_{ss}[\theta] = \lim_{t \rightarrow \infty} P[\theta, t]$ , we consider the solution of  $\partial_t P[\theta, t] = 0$  that is

$$P_{ss}[\theta] = \det M \exp \left( -\frac{H_{xy}[\theta]}{T} - \frac{\tau}{2T} |\nabla_{\theta_i} H_{xy}|^2 \right) \cdot Z_{eff}^{-1}, \quad (9)$$

the numerical constant  $Z_{eff}^{-1}$  is the normalization factor. According to (9), we can write an effective free energy  $F_{eff}(T, \tau)$ . The thermodynamics is then given by the following equations

$$\begin{aligned} F_{eff}(N, T, \tau) &= -T \ln Z_{eff} \\ Z_{eff} &\equiv \int_0^{2\pi} \prod_i d\theta_i e^{-\frac{1}{T} H_{eff}[\theta]} \\ H_{eff}[\theta] &\equiv H_{xy}[\theta] + \frac{\tau}{2} |\nabla_{\theta_i} H_{xy}|^2 - T \ln \det M. \end{aligned} \quad (10)$$

The presence of  $\det M$  in (10) makes the effective free energy calculation a hard task that needs further approximations. As we have discussed before, UCNA holds in the limits  $\tau \rightarrow 0$  and  $\tau \rightarrow \infty$ . In the first case, even in the presence of negative curvatures, the term  $\delta_{ij}$  dominates with respect the Hessian matrix  $\frac{\partial^2 H_{xy}}{\partial \theta_i \partial \theta_j}$ . In that situation the determinant can be computed analytically considering the Hessian as a small perturbation to the identity matrix. The mean-field model, i. e.,  $d = \infty$ , will be addressed in Sec. III considering a fully connected lattice model  $J_{ij} = J/N$ . In this way one can compute

analytically the partition function in the small  $\tau$  limit. After that, in Sec. IV, we will study the model for  $d = 2$  in the continuum limit, i. e., the spin-wave approximation of  $H_{xy}$ . In two dimension,  $J_{ij}$  is different from zero only between nearest neighbor sites.

### III. MEAN FIELD APPROXIMATION AND LANDAU-GINZBURG FREE ENERGY

Here we are interested in investigating the critical properties of  $xy$ -model, i. e., the properties of the system near a second order phase transition. To do so, we neglect the spatial properties of the system performing the computation (10) on a fully-connected lattice. In this way, we can analytically compute the partition function and also write the corresponding Landau-Ginzburg theory. The fully connected lattice is obtained considering an adjacent matrix  $J_{ij} = J/N$ . We compute the effective thermodynamics (10) performing a saddle-point approximation to evaluate the partition function  $Z_{eff}$  (see Appendix A). Introducing the free-energy per spin  $f(T, \tau) = F_{eff}(N, T, \tau)/N$  and the inverse temperature  $\beta = 1/T$ , one has

$$f[m] = \frac{\beta J}{2} \left( 1 + \frac{\tau J}{2} \right) m^2 - \ln z[m] \quad (11)$$

$$z[m] \equiv I_0(\beta J m) + \tau m I_1(\beta J m),$$

where  $m$  is the modulus of the magnetization  $\mathbf{m} = (m_x, m_y) = \langle N^{-1} \sum_i \mathbf{s}_i \rangle$ . We have indicated with  $I_n(x)$  the modified Bessel function of order  $n$ . It is worth noting that (11) holds only in the small tau limit where we can write  $\det M \sim 1 + \tau \text{Tr} \partial_{\theta_i, \theta_j}^2 H_{xy}$ . By minimizing with respect  $m$ , we obtain the self-consistency equations

$$m - \frac{[2I_1(\beta J m) + \tau J (I_0(\beta J m) + I_2(\beta J m))]}{2z} = 0. \quad (12)$$

As one can check, when  $\tau = 0$ , the equation reduces to the well known mean-field result  $m(\beta) = I_1(\beta J m)/I_0(\beta J m)$ . By expanding (11) up to the fourth order in  $m$  and recalling that  $m$  is the modulus of the magnetization  $\mathbf{m} = (m_x, m_y)$ , we obtain the following Landau-Ginzburg free energy

$$f_{LG}[m_x, m_y] = \frac{A}{2}(m_x^2 + m_y^2) + \frac{B}{4}(m_x^2 + m_y^2)^2 \quad (13)$$

$$A \equiv J\beta \left[ 1 - \frac{J}{2}(\tau + \beta) \right]$$

$$B \equiv \frac{J^4 \beta^2}{8} \left[ \frac{\beta^2}{2} + \tau \left( \frac{1}{2} + \tau\beta \right) \right].$$

$f_{LG}$  contains all the information we need to understand the critical properties of the system in mean-field approximation. For instance, writing  $m = |\mathbf{m}|$  and considering the solution

$$\frac{\partial f_{LG}}{\partial m} = 0, \quad \frac{\partial^2 f_{LG}}{\partial m^2} > 0 \quad (14)$$

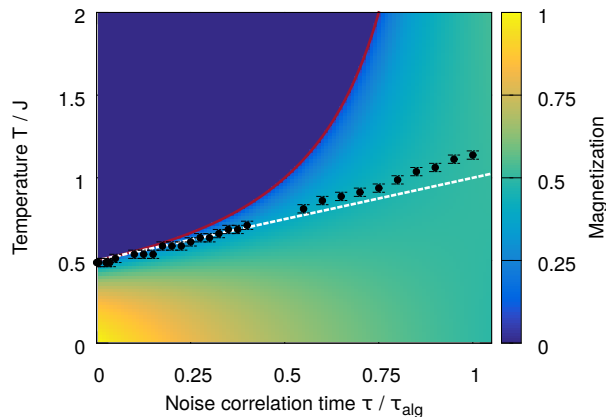


FIG. 1. Phase diagram. Mean field phase diagram obtained minimizing the free energy (11). The red curve is the analytical computation of the critical line given by (15), black symbols are numerical simulations, white dashed curve is the small  $\tau$  expansion of (15).

we obtain the spontaneous magnetization  $m_s$ . In the symmetry broken phase one has  $m_s = \sqrt{-A/B}$ . According to Eq. (13), the Goldstone picture remains untouched. To realize that we write  $\mathbf{m}$  as a complex field parametrized through two real fields  $\varphi_1$  and  $\varphi_2$ , i. e.,  $\mathbf{m} \rightarrow \varphi_1 + i\varphi_2$ . Looking at the fluctuations near to the minimum of  $f_{LG}$ , in the symmetry broken phase, we can write  $\varphi_1 = m_s + \delta\varphi_1$  and  $\varphi_2 = \delta\varphi_2$ . Inserting these two expressions in  $f_{LG}$ , one obtains that  $m_s^2$  is the mass of the longitudinal fluctuation  $\delta\varphi_1$  while the transverse mode  $\delta\varphi_2$  is massless, i. e., the Goldstone mode.

To estimate the critical line  $T_{mf}(\tau)$  one has to consider the solution of the equation  $A = 0$  that is

$$\frac{T_{mf}(\tau)}{J} = \frac{1}{2 - \tau J} \simeq \frac{1}{2} \left[ 1 + \frac{\tau J}{2} \right]. \quad (15)$$

As we show in (A 2), the same critical line can be computed from the free-energy  $f[m]$  given by (11). According to (15), we notice that  $T_{mf}(\tau)$  increases with  $\tau$  and diverges when  $\tau = 2/J \equiv \tau_{alg}$ . Here, we have introduced a characteristic time scale  $\tau_{alg}$  that is the time needed to align a spin with the resulting mean-field acting on it. Since the computation holds at small  $\tau$ , the divergence is unphysical. Thus, we have to consider the small  $\tau$  expansion of  $T_{mf}(\tau)$ .

In Fig. (1) we show the resulting phase diagram obtained by minimizing numerically the free energy (11). The contour plot represents the magnetization  $m(\tau/\tau_{alg}, T)$ . The red curve is the critical line (15), the black symbols are obtained by numerical simulations of the fully-connected lattice, the details of numerical simulations are in Sec. (D). As one can see, the theoretical prediction reproduces quite well the numerical simulations in the small  $\tau$  limit, to highlight this finding we

have plotted in white the small  $\tau$  expansion. However, deviations from the approximated theory become dramatic by increasing  $\tau$ .

#### IV. TOPOLOGICAL TRANSITION IN TWO DIMENSIONS

In this section, we discuss the effect of persistent noise in  $d = 2$  where BKT transition takes place at temperature  $T_{BKT}$  for  $\tau = 0$ . To do so, we start with considering  $H_{xy}$  in the spin-wave approximation [1] that is

$$H[\theta(\mathbf{r})] = \frac{J}{2a^{d-2}} \int d^d r \nabla\theta(\mathbf{r}) \cdot \nabla\theta(\mathbf{r}), \quad (16)$$

where  $a$  is the lattice spacing. To write the equation of motion for  $\theta(\mathbf{r})$ , we introduce an auxiliary field  $\psi(\mathbf{r})$  undergoing an Ornstein-Uhlenbeck process

$$\dot{\theta}(\mathbf{r}) = -\frac{\delta H[\theta]}{\delta\theta(\mathbf{r})} + \psi(\mathbf{r}) \quad (17)$$

$$\tau\dot{\psi}(\mathbf{r}) = -\psi(\mathbf{r}) + \sqrt{T}\eta(\mathbf{r}),$$

the noise term satisfies  $\langle\eta(\mathbf{r})\rangle = 0$  and  $\langle\eta(\mathbf{r}, t)\eta(\mathbf{r}', s)\rangle = 2\delta(\mathbf{r} - \mathbf{r}')\delta(t - s)$ . By introducing the rescaled time  $z = \tau^{-1/2}t$ , we can write

$$\ddot{\theta}(\mathbf{r}) = -\dot{\theta}(\mathbf{r})\tilde{M}[\theta(\mathbf{r})] - \frac{\delta H}{\delta\theta(\mathbf{r})} + \tilde{\eta}(\mathbf{r}, z) \quad (18)$$

$$\tilde{M}[\theta(\mathbf{r})] \equiv \frac{1}{\tau^{1/2}} + \tau^{1/2} \frac{\delta^2 H}{\delta\theta(\mathbf{r})\delta\theta(\mathbf{r}' )}$$

where for the noise term  $\tilde{\eta}(\mathbf{r}, z)$  one has  $\langle\tilde{\eta}(\mathbf{r}, z)\rangle = 0$  and  $\langle\tilde{\eta}(\mathbf{r}, z)\tilde{\eta}(\mathbf{r}', z')\rangle = 2T\tau^{-1/2}\delta(\mathbf{r} - \mathbf{r}')\delta(z - z')$ . In the large friction limit  $\tilde{M} \gg 1$ , we can neglect the inertial term  $\ddot{\theta}(\mathbf{r}) \rightarrow 0$ . Since the continuum approximation is performed around the ground state, i. e., where the system is locally stable, the overdamped dynamics is recovered in the limit  $\tau \rightarrow 0$  and  $\tau \rightarrow \infty$ . Here, we will consider the limit  $\tau \rightarrow 0$ , meaning that our results are valid only in the small  $\tau$  limit. In that limit and at small enough temperature, the equation of motion for  $\theta(\mathbf{r})$  reads

$$\dot{\theta}(\mathbf{r}) = -\frac{\delta H_{eff}}{\delta\theta(\mathbf{r})} \quad (19)$$

where we have introduced the effective Hamiltonian

$$H_{eff}[\theta(\mathbf{r})] = H + H_1 \quad (20)$$

$$H_1 \equiv \frac{\tau J^2}{2a^{d-4}} \int d^d r (\Delta\theta(\mathbf{r}))^2.$$

It is convenient to express  $\theta(\mathbf{r})$  in terms of its Fourier components  $\theta(\mathbf{r}) = N^{-1/2} \sum_{\mathbf{k}} \theta_{\mathbf{k}} e^{i\mathbf{k}\cdot\mathbf{r}}$ . In this way, we can rewrite the energy as

$$H_{eff}[\theta] = \frac{a^2 J}{2} \sum_{\mathbf{k}} k^2 \theta_{\mathbf{k}} \theta_{-\mathbf{k}} + \frac{\tau a^4 J^2}{2} \sum_{\mathbf{k}} k^4 \theta_{\mathbf{k}} \theta_{-\mathbf{k}} \quad (21)$$

with  $k = |\mathbf{k}|$ . As well as the BKT case, we can write  $\theta(\mathbf{r}) = \theta_{sw}(\mathbf{r}) + \theta_v(\mathbf{r})$ , where  $\theta_{sw}$  is the spin wave configuration and  $\theta_v$  the vortex configuration.

Now, we can compute the spin-spin correlation function  $g(r) = \langle e^{-i[\theta_{sw}(\mathbf{r}) - \theta_{sw}(0)]} \rangle$ , the details are discussed in Appendix C. In the limit  $r^2 \gg a^2 J\tau$  one has

$$g(r) \sim \left(\frac{\pi r}{a}\right)^{-\frac{T}{2\pi J}} (1 + J\pi\tau)^{\frac{T}{4\pi J}}. \quad (22)$$

Because  $g(r \rightarrow \infty) = 0$ , Eq. (22) implies also that, as well the equilibrium case, no long-range order is found for an infinite system. However, for a finite-size system, if  $r$  is of the order of the system size and  $a^2 J\tau \gg r^2$ , we have that  $g(r) \simeq 1$ , i. e., the system is practically in the ground state with all the spins aligned. In other words, at low enough temperatures, memory in the noise promotes uniform configuration suppressing long wave length excitations, at least in the small  $\tau$  regime. To check the validity of that prediction, we have computed numerically the spin-spin correlation function  $g(r)$ , the details of the simulations are given in Appendix D. In particular, we have fitted the numerical data to the functional form  $g_{fit}(r) = (Ar)^{-T/B} (1 + \frac{B\tau}{2})^{T/2B}$ . In Fig. (2-a) we show the behavior of  $T/B$  vs  $T$  for  $\tau = 0.01, 0.05, 0.1$ , squares, circles, and triangles, respectively. The black line is the theoretical prediction (22), i. e.,  $B = 2\pi J$ . As one can see, for temperatures  $T < 0.5$ , the data collapse on (22).

Now we estimate the energy cost of a single vortex in the presence of correlated noise. In this way, we can quantify the effect of persistent noise on the BKT temperature. The vortex configurations  $\theta_v(\mathbf{r})$  minimize (20) and satisfy the boundary condition  $\oint d\mathbf{l} \cdot \nabla\theta_v = 2n\pi$ . As well in the equilibrium case, also in the small  $\tau$  limit, vortices have the form  $\nabla_{\tau}\theta_v(r) = 1/r$ . Inserting the vortex configuration in  $H_{eff}$ , we can compute the free energy cost  $\Delta f_{vortex} = H - k_B T S$ , where  $S$  is the entropy of a single vortex. Performing a straightforward calculation, one can obtain  $\Delta f_{vortex}$  that is

$$\begin{aligned} \Delta f_{vortex} &= H_0 + H_1 - 2k_B T \ln \frac{L}{a} \quad (23) \\ &= [\pi J - 2k_B T] \ln \frac{L}{a} \\ &\quad + \frac{\pi\tau J^2}{2} \left[ 1 - \frac{a^2}{L^2} \right]. \end{aligned}$$

According to (23), the exponentially correlated noise produces a shift  $\Delta T_{BKT}$  in the critical temperature of the topological transition that is

$$\Delta T_{BKT}(\tau) = \frac{\pi J^2 g(L, a)}{4 \ln(L/a)} \tau \quad (24)$$

$$g(L, a) \equiv 1 - \frac{a^2}{L^2}.$$

As one can see,  $\Delta T_{BKT}$  is linear in  $\tau$ . However, since the linear size of the system  $L$  grows with  $N^{1/2}$ , in the thermodynamic limit  $\lim_{N \rightarrow \infty} \Delta T_{BKT} = 0$ , meaning that the

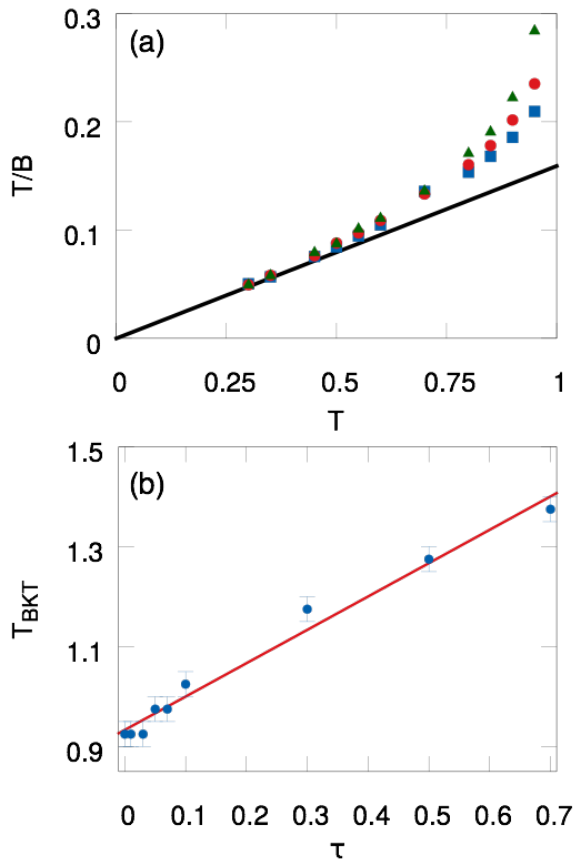


FIG. 2. Two dimensional simulations. (a) Comparison between theory (22) and numerical simulations. Triangles, circles and squares are  $\tau = 0.01, 0.05, 0.1$ , respectively. At small temperatures  $T < 0.5$ , data collapse on the same curve. (b) Monotonic shift in the temperature of the topological transition as a function of  $\tau$ . Blue symbols are simulations, the red line is the linear fit  $T_{BKT}(\tau) = a + b\tau$ , with  $a = 0.93(1)$  and  $b = 0.67(3)$ .

location of the topological transition remains untouched. Considering a finite size system, we can define a size-dependent crossover temperature  $T_{BKT}(\tau, N)$ . According to (24), one has  $\lim_{N \rightarrow \infty} T_{BKT}(\tau, N) = T_{BKT}$ . However, at finite  $N$ , we expect to observe a linear shift in  $\tau$  towards higher temperature. We have tested that prediction in numerical simulations. The resulting shift in  $T_{BKT}$  is shown in Fig. (2-b). As one can see, it is in good agreement with (24). The blue line is obtained fitting the data to  $T_{BKT}(N, \tau) = a + b\tau$ , where  $a$  and  $b$  are the fitting parameters. The parameter  $a \equiv T_{BKT}(0) \sim 0.9$  is compatible with recent accurate estimate of  $T_{BKT}$  [25, 26].

## V. SUMMARY AND DISCUSSION

In this paper, we have proposed an effective equilib-

rium theory for the  $xy$ -model driven out-of-equilibrium by exponentially correlated noise. To map the original many-body problem into an effective equilibrium picture, we have employed UCNA [9, 21]. In the results presented here, the persistent time  $\tau$  plays the role of external and tunable thermodynamic parameter. Moreover, even though UCNA should work also in the  $\tau \rightarrow \infty$  limit, in the many-body case the presence of  $\det M$  requires, in general, further approximations [10]. Since the matrix  $M$  has the form  $M = \mathbb{1} + \tau\mathbb{H}$ , where  $\mathbb{1}$  is the identity matrix and  $\mathbb{H}$  the Hessian matrix, we have considered the approximation  $\det M = 1 + \tau \text{Tr} \mathbb{H}$ , that holds in the small  $\tau$  limit. We have specialized our computation in two cases: (i)  $d = \infty$  corresponding to the mean-field approximation, and (ii)  $d = 2$ , where, in equilibrium, BKT transition takes place. Differently from the scalar field case, where a Landau  $\varphi^4$  theory has been proposed phenomenologically to describe the impact of correlated noise on critical phenomena in Active Matter [12], the mean-field computation presented here allows to obtain the coarse-grained theory starting from a microscopical model. In particular, we have computed analytically the effective partition function and, expanding the free energy around the transition point, we have obtained the corresponding Landau-Ginzburg free energy  $f_{LG}$ .

We have shown that the coefficient of the quadratic term of  $f_{LG}$  vanishes along the critical line  $T_{mf}(\tau)$ . Moreover, the resulting  $T_{mf}(\tau)$  is an increasing function of  $\tau$ , i. e., starting from a disorder configuration at high  $T$  and maintaining  $T$  fixed, the memory of the noise can be tuned to bring the system at criticality. This property of non-equilibrium models driven by exponentially correlated noise seems to be quite general since it has been already observed in both, theory and numerical simulations in the case of zero-dimensional  $\varphi^4$  theory with exponentially correlated noise [12], i. e., the gas-liquid universality class, and also in the case of the glassy transition of active particles driven by colored noise [27–29].

To check the validity of that finding we have performed numerical simulations of the fully-connected model. The critical points in the small  $\tau$  regime obtained from numerical simulations follow quite well the theoretical prediction  $T_{mf}(\tau)$ . Since  $f_{LG}$  describes an  $O(2)$  vectorial field theory, crossing the critical line the symmetry  $O(2)$  is spontaneously broken and, according to the Goldstone mechanism [30], the longitudinal fluctuations are massless, while the mass of the transverse excitation depends on  $\tau$ .

After that, we have studied the theory in two dimensions where BKT transition takes place. We have shown that, in the small  $\tau$  limit, the topological transition remains untouched by the non-equilibrium dynamics. However, considering a finite size system, the theory predicts a linear shift in  $T_{BKT}$  meaning that memory disadvantages vortex excitations. Thus, at low temperatures, the non-equilibrium system turns to be more correlated than the equilibrium counterpart. Performing numerical simulations in two dimensions, we found a good qualitative

agreement between theory and numerics.

It would be very interesting to try to extend these approximation schemes to off-lattice models. In this way, one could estimate the impact of memory effects on the collective properties of assemblies of self-propelled particles with alignment interactions [15]. Recently, it has been shown in both experiments and models, that memory effects in the angular dynamics play an important role [18, 19]. It is worth noting that the well established methods describing collective properties of self-propelled particles can not be applied in the case of exponentially correlated dynamics [14]. For instance, analytical predictions about the effects of exponentially correlated noise on angular dynamics can be made only in the low-density limit and considering a simplified one-dimensional telegraphic noise model for describing the memory effects [18]. According to our computation scheme, in the small  $\tau$  limit, memory effects in the angular dynamics can be reabsorbed into an effective equilibrium Hamiltonian  $H_{eff} = H_{xy} + \frac{J\tau}{2} |\nabla_{\theta} H_{xy}|^2$ .

## ACKNOWLEDGMENTS

We thank M. Cristina Marchetti for illuminating discussions and S. Roldán Vargas for his critical reading of the manuscript, MP was supported by the Simons Foundation Targeted Grant in the Mathematical Modeling of Living Systems Number: 342354 and by the Syracuse Soft Matter Program. C. Maggi acknowledges support from the European Research Council under the European Union's Seventh Framework programme (FP7/2007-2013)/ERC Grant agreement No. 307940.

## Appendix A: Fully connected model

The mean-field solution of the  $xy$ -model has been computed considering a fully-connected lattice that corresponds to  $d = \infty$  situation [11, 31, 32]. The Hamiltonian reads

$$H_{xy}^{MF}[\theta] = -\frac{J}{2N} \sum_{i,j} \cos(\theta_i - \theta_j). \quad (\text{A1})$$

To compute the partition function we introduce the following order parameters

$$\begin{aligned} N\phi &= \sum_i \cos \theta_i, & N\psi &= \sum_i \sin \theta_i \\ N\pi &= \sum_i \cos 2\theta_i, & N\sigma &= \sum_i \sin 2\theta_i, \end{aligned} \quad (\text{A2})$$

in terms of the order parameters the Hamiltonian can be written as follows

$$\begin{aligned} H_{xy}^{MF}[\theta] &= -\frac{NJ}{2} \left(1 - \frac{\tau J}{2}\right) [\phi^2 + \psi^2] + \\ &+ \frac{N\tau J^2}{4} (\psi^2 - \phi^2) \pi + \\ &- \frac{N\tau J^2}{2} \phi\psi\sigma - \frac{1}{\beta} \ln \det M. \end{aligned} \quad (\text{A3})$$

In the small  $\tau$  limit, we approximate the determinant in the following way

$$\det M \simeq 1 + \tau Tr \frac{\partial^2 H_{xy}^{MF}}{\partial \theta_i \partial \theta_j} \quad (\text{A4})$$

and the trace of the Hessian matrix reads

$$Tr \frac{\partial^2 H_{xy}^{MF}}{\partial \theta_i \partial \theta_j} = J \sum_i (\phi \cos \theta_i + \psi \sin \theta_i) + \mathcal{O}\left(\frac{1}{N}\right). \quad (\text{A5})$$

To compute the partition function we represent the order parameters  $(\phi, \psi, \pi, \sigma)$  through a set of lagrangian multipliers  $\lambda_k$ , with  $k = 1, \dots, 4$ , as follows

$$\begin{aligned} \delta \left( N\phi - \sum_i \cos \theta_i \right) &= \int d\lambda_1 e^{-\lambda_1 (N\phi - \sum_i \cos \theta_i)} \\ \delta \left( N\psi - \sum_i \sin \theta_i \right) &= \int d\lambda_2 e^{-\lambda_2 (N\psi - \sum_i \sin \theta_i)} \\ \delta \left( N\pi - \sum_i \cos 2\theta_i \right) &= \int d\lambda_3 e^{-\lambda_3 (N\pi - \sum_i \cos 2\theta_i)} \\ \delta \left( N\sigma - \sum_i \sin 2\theta_i \right) &= \int d\lambda_4 e^{-\lambda_4 (N\sigma - \sum_i \sin 2\theta_i)} \end{aligned}$$

finally, the partition function reads

$$Z = \mathcal{N} \int d\Phi e^{-Nf}, \quad \Phi \equiv (\lambda_i, \phi, \psi, \pi, \sigma) \quad (\text{A6})$$

$$\begin{aligned} f &\equiv -\frac{\beta J}{2} \left(1 - \frac{\tau J}{2}\right) (\phi^2 + \psi^2) + \\ &+ \frac{\beta J^2 \tau}{4} (\psi^2 - \phi^2) \pi - \frac{1}{2} \beta J^2 \tau \phi\psi\sigma + \\ &+ \lambda_1 \phi + \lambda_2 \psi + \lambda_3 \pi + \lambda_4 \sigma - \log z \\ z &\equiv \int_0^{2\pi} d\theta A(\phi, \psi)_{\theta} e^{-\mathcal{H}'} \end{aligned}$$

$$A(\phi, \psi)_{\theta} \equiv 1 + \tau J (\phi \cos \theta + \psi \sin \theta)$$

$$-\mathcal{H}' \equiv \lambda_1 \cos \theta + \lambda_2 \sin \theta + \lambda_3 \cos 2\theta + \lambda_4 \sin 2\theta$$

where  $\mathcal{N}$  is a normalization constant.

### 1. Saddle-point equations

In the thermodynamic limit  $N \rightarrow \infty$ , we can perform the saddle-point approximation to evaluate the partition

function [11, 31, 32]

$$Z \sim e^{-Nf_{SP}}, \quad \left. \frac{\partial f}{\partial \Phi} \right|_{SP} = 0 \quad (\text{A7})$$

and the saddle-point equations are

$$\begin{aligned} \lambda_1 &= \frac{\beta J^2 \tau}{2} (\phi\pi + \psi\sigma) + \beta J \left(1 - \frac{\tau J}{2}\right) \phi + I_1 \\ \lambda_2 &= \frac{\beta J^2 \tau}{2} (\phi\sigma - \psi\pi) + \beta J \left(1 - \frac{\tau J}{2}\right) \psi + I_2 \\ \lambda_3 &= \frac{\beta J^2 \tau}{4} (\phi^2 - \psi^2) \\ \lambda_4 &= \frac{1}{2} \beta J^2 \tau \phi \psi \\ \phi &= \langle \cos \theta \rangle_{\mathcal{H}}, \quad \psi = \langle \sin \theta \rangle_{\mathcal{H}} \\ \pi &= \langle \cos 2\theta \rangle_{\mathcal{H}}, \quad \sigma = \langle \sin 2\theta \rangle_{\mathcal{H}} \\ -\mathcal{H} &\equiv -\mathcal{H}' + \log A(\phi, \psi)_{\theta} \\ I_1 &\equiv \frac{\tau J}{z} \int d\theta \cos \theta e^{-\mathcal{H}'} \\ I_2 &\equiv \frac{\tau J}{z} \int d\theta \sin \theta e^{-\mathcal{H}'} \end{aligned} \quad (\text{A8})$$

where we have introduced the average of a generic observable with respect the effective one-body Hamiltonian  $\mathcal{H}$  that is  $\langle \mathcal{O} \rangle_{\mathcal{H}} \equiv \frac{\int d\theta \mathcal{O} e^{-\mathcal{H}}}{\int d\theta e^{-\mathcal{H}}}$ .

## 2. Elimination of the redundant variables

In order to eliminate the redundant variables that we have introduced to compute the partition function, we write the auxiliary fields in polar coordinates

$$\begin{aligned} \phi &= m \cos \Theta, \quad \lambda_1 = \Lambda \cos \lambda, \quad \lambda_3 = n \cos \hat{\lambda} \\ \psi &= m \sin \Theta, \quad \lambda_2 = \Lambda \sin \lambda, \quad \lambda_4 = n \sin \hat{\lambda} \end{aligned} \quad (\text{A9})$$

From the equations for  $\lambda_{3,4}$  it follows that  $n = \hat{\lambda} = 0$ , and, as a consequence,  $\pi = \sigma = 0$ . The free energy of the model can be written as follows

$$\begin{aligned} f[m, \Lambda] &= -\frac{\beta J}{2} \left(1 - \frac{\tau J}{2}\right) m^2 + m\Lambda - \log z \\ z &= I_0(\Lambda) + \tau J m I_1(\Lambda). \end{aligned} \quad (\text{A10})$$

The self-consistency equations are

$$\begin{aligned} \frac{\partial f}{\partial m} &= -\beta J \left(1 - \frac{\tau J}{2}\right) m + \Lambda - \frac{\tau J I_1(\Lambda)}{z} = 0 \\ \frac{\partial f}{\partial \Lambda} &= m - \frac{1}{2z} [2I_1(\Lambda) + \tau J (I_0(\Lambda) + I_2(\Lambda))] = 0. \end{aligned} \quad (\text{A11})$$

When  $\tau = 0$  we recover the mean field solution of the equilibrium  $xy$  model

$$\begin{aligned} \Lambda &= \beta J m \\ m &= \frac{I_1(\beta J m)}{I_0(\beta J m)} \end{aligned} \quad (\text{A12})$$

Moreover, from (A11) one has  $\Lambda = \beta J m + \mathcal{O}(\tau^2)$ . Plugging this relation in (A10) we obtain (11). The critical line  $T_{mf}(\tau)$  can be computed considering the solution of  $\partial_m^2 f[m] \big|_{m=0} = 0$ . The computation brings to the same result obtained in the main text (15) that has been obtained considering the Landau-Ginzburg free energy (13).

## Appendix B: Spin waves

At low enough temperature the  $xy$  Hamiltonian in  $d$  spatial dimensions can be written as follows

$$H = \frac{J}{2a^{d-2}} \int d^d r \nabla \theta(r) \cdot \nabla \theta(r). \quad (\text{B1})$$

As we have shown in the main text, the effective Hamiltonian in the small noise limit reads

$$H_{eff} \equiv H + \frac{\tau}{2} \left| \frac{\delta H}{\delta \theta} \right|^2. \quad (\text{B2})$$

Now, to evaluate the second term on the left-hand side of the last equation, we come back to the lattice model. When  $d < \infty$ ,  $J_{i,j} = J \neq 0$  only for nearest neighbor sites  $i, j$  that we indicate  $\langle i, j \rangle$ . The Hamiltonian reads

$$H = -J \sum_{\langle i, j \rangle} \cos(\theta_i - \theta_j) \simeq -J \sum_{\langle i, j \rangle} \left[ 1 - \frac{(\theta_i - \theta_j)^2}{2} \right] \quad (\text{B3})$$

the derivative with respect  $\theta_i$  reads

$$\frac{\partial H}{\partial \theta_i} = -J \sum_i (\theta_{i+a} + \theta_{i-a} - 2\theta_i) = -Ja^2 \Delta \theta_i \quad (\text{B4})$$

where  $\Delta$  is the Laplace operator. In the continuum limit the Hamiltonian becomes

$$\begin{aligned} H_{eff} &= H + H_1 \\ H_1 &\equiv \frac{\tau J^2}{2a^{d-4}} \int d^d r (\Delta \theta(\mathbf{r}))^2. \end{aligned} \quad (\text{B5})$$

## Appendix C: Spin-spin correlation function

Now we compute the spin-spin correlation function  $g(r)$  that is [1]

$$g(r) = \exp \left\{ -\frac{1}{2} \int \prod_{\mathbf{k}} d\theta_{\mathbf{k}} e^{-\frac{H_{eff}}{T}} [\theta(\mathbf{r}) - \theta(0)]^2 \right\} \quad (\text{C1})$$

which is

$$g(r) = \frac{T}{N} \sum_{\mathbf{k}} \frac{1 - \cos(\mathbf{k} \cdot \mathbf{r})}{a^2 J k^2 + a^4 J k^4 \tau}. \quad (\text{C2})$$

Now we switch to the continuum also in  $k$ -space by setting  $N^{-1} \sum_{\mathbf{k}} \dots \rightarrow \frac{a^d}{(2\pi)^d} \int d\mathbf{k} \dots$  so that Eq. (C2) becomes

$$g(r) = T \left( \frac{a}{2\pi} \right)^d \int d\mathbf{k} \frac{1 - \cos(\mathbf{k} \cdot \mathbf{r})}{a^2 J k^2 + a^4 J k^4 \tau}. \quad (\text{C3})$$

Specializing the calculation to  $d = 2$  case, by integrating Eq. (C3) in polar coordinates, introducing the Bessel function  $J_0(x)$ , we get

$$g(r) = T \left( \frac{a}{2\pi} \right)^2 \int dk 2\pi k \frac{1 - J_0(kr)}{a^2 Jk^2 + a^4 Jk^4 \tau}. \quad (\text{C4})$$

When  $r$  is very large compared with  $a$ , we can neglect the Bessel function and approximate Eq. (C4) as

$$g(r) \simeq \frac{\pi r^{-\frac{T}{2\pi J}}}{a} \left[ \frac{r^2 + a^2 J \tau}{r^2 (1 + J \pi \tau)} \right]^{-\frac{T}{4\pi J}} \quad (\text{C5})$$

when  $r^2 \gg a^2 J \tau$ , we recover the result Eq. (22) of the main text.

#### Appendix D: Numerical simulations

We have solved numerically the equations of motion (4) where the  $N$  compasses  $\mathbf{s}_{\mathbf{r}} = (\cos \theta_{\mathbf{r}}, \sin \theta_{\mathbf{r}})$  are arranged on a two dimensional square lattice. The vector  $\mathbf{r}$  with  $\mathbf{r} = i\mathbf{x} + j\mathbf{y}$  individuates the site  $(i, j)$  of the lattice, with  $i, j = 1, \dots, \sqrt{N}$ . The connectivity of the adjacent matrix  $J_{ij}$  defines the spatial dimensions  $d$  where the model is embedded. In finite dimensions  $d$ ,  $J_{ij} = J$  among nearest neighbor sites. The mean-field consists in a fully-connected lattice, i. e.,  $J_{ij} = J/N, \forall i, j$ . Here, we report the results concerning  $N = 4900$  ( $d = 2$ ) and  $N = 400$

(fully-connected lattice). The equations of motion are integrated using a second-order Runge-Kutta scheme with integration time step  $dt = 10^{-3}$ .

#### 1. Two dimensions

In two dimensions, we have computed the correlation function

$$g(\mathbf{r}) = \left\langle N^{-1} \sum_{\mathbf{r}'} \mathbf{s}_{\mathbf{r}+\mathbf{r}'} \cdot \mathbf{s}_{\mathbf{r}'} \right\rangle_t, \quad (\text{D1})$$

where the average  $\langle \cdot \rangle_t$  in (D1) of a generic observable  $\mathcal{O}[\theta(t)]$  is computed averaging over one long trajectory of the system with a single noise realization, i. e.,  $\langle \mathcal{O} \rangle_t = t^{-1} \int_{t_0}^{t_0+t} ds \mathcal{O}[\theta(s)]$ .

The transition temperature  $T_{BKT}(\tau)$  has been computed considering a power law fit to  $r^{-\eta}$  for the spatial correlation function  $g(r)$ . We define  $T_{BKT}(\tau)$  using the criterium  $\eta = \frac{1}{4}$  at the transition temperature [33].

#### 2. Mean Field

In Fig. (1), we compare the mean-field prediction (15) with numerical simulations of a fully-connected lattice composed by  $N = 400$ . We have considered 30 temperatures for each  $\tau$  with  $\tau \in [10^{-3}, 2]$ . The critical point has been obtained considering the modulus of the magnetization  $m = \sqrt{m_x^2 + m_y^2}$ , where  $m_x = N^{-1} \sum_{\mathbf{r}} \cos \theta_{\mathbf{r}}$ , and  $m_y = N^{-1} \sum_{\mathbf{r}} \sin \theta_{\mathbf{r}}$  are the magnetization along  $x$  and  $y$ , respectively. To evaluate the transition temperature, we have looked at the susceptibility  $\chi = N \langle (m - \langle m \rangle)^2 \rangle$  that develops a peak at the transition.

- 
- [1] M. Plischke and B. Bergersen, *Equilibrium statistical physics* (World Scientific Publishing Co Inc, 1994).
  - [2] S.-K. Ma, *Statistical Mechanics* (World Scientific, 1985).
  - [3] N. D. Mermin and H. Wagner, Phys. Rev. Lett. **17**, 1133 (1966).
  - [4] S. Coleman, Communications in Mathematical Physics **31**, 259 (1973).
  - [5] P. C. Hohenberg, Phys. Rev. **158**, 383 (1967).
  - [6] V. Berezinskii, Sov. Phys. JETP **32**, 493 (1971).
  - [7] V. Berezinskii, JETP **32**, 34 (1970).
  - [8] J. M. Kosterlitz and D. J. Thouless, Journal of Physics C: Solid State Physics **6**, 1181 (1973).
  - [9] P. Jung and P. Hänggi, Phys. Rev. A **35**, 4464 (1987).
  - [10] C. Maggi, U. M. B. Marconi, N. Gnan, and R. Di Leonardo, Scientific reports **5** (2015).
  - [11] G. Parisi, *Statistical field theory* (Addison-Wesley, 1988).
  - [12] M. Paoluzzi, C. Maggi, U. Marini Bettolo Marconi, and N. Gnan, Phys. Rev. E **94**, 052602 (2016).
  - [13] C. Bechinger, R. Di Leonardo, H. Löwen, C. Reichhardt, G. Volpe, and G. Volpe, Rev. Mod. Phys. **88**, 045006 (2016).
  - [14] M. C. Marchetti, J. F. Joanny, S. Ramaswamy, T. B. Liverpool, J. Prost, M. Rao, and R. A. Simha, Rev. Mod. Phys. **85**, 1143 (2013).
  - [15] T. Vicsek and A. Zafeiris, Physics Reports **517**, 71 (2012).
  - [16] M. E. Cates, Reports on Progress in Physics **75**, 042601 (2012).
  - [17] F. Vega Reyes and A. Lasanta, Entropy **19** (2017).
  - [18] K. H. Nagai, Y. Sumino, R. Montagne, I. S. Aranson, and H. Chaté, Phys. Rev. Lett. **114**, 168001 (2015).
  - [19] Y. Sumino, K. H. Nagai, Y. Shitaka, D. Tanaka, K. Yoshikawa, H. Chaté, and K. Oiwa, Nature **483**, 448 (2012).
  - [20] J. A. Acebrón, L. L. Bonilla, C. J. Pérez Vicente, F. Ritort, and R. Spigler, Rev. Mod. Phys. **77**, 137 (2005).
  - [21] P. Hänggi and P. Jung, Advances in chemical physics **89**, 239 (1995).
  - [22] U. M. B. Marconi and C. Maggi, Soft matter **11**, 8768 (2015).

- [23] U. M. B. Marconi, N. Gnan, M. Paoluzzi, C. Maggi, and R. Di Leonardo, *Scientific reports* **6**, 23297 (2016).
- [24] U. M. B. Marconi, M. Paoluzzi, and C. Maggi, *Molecular Physics* **114**, 2400 (2016).
- [25] M. I. Berganza and L. Leuzzi, *Physical Review B* **88**, 144104 (2013).
- [26] M. Hasenbusch, *Journal of Physics A: Mathematical and General* **38**, 5869 (2005).
- [27] G. Szamel, E. Flenner, and L. Berthier, *Physical Review E* **91**, 062304 (2015).
- [28] S. K. Nandi and N. S. Gov, arXiv preprint arXiv:1605.06073 (2016).
- [29] S. K. Nandi and N. S. Gov, *Soft matter* **13**, 7609 (2017).
- [30] J. Goldstone, *Il Nuovo Cimento (1955-1965)* **19**, 154 (1961).
- [31] J. Zinn-Justin, *Quantum field theory and critical phenomena* (Clarendon Press, 1996).
- [32] M. Mézard, G. Parisi, and M. Virasoro, *Spin glass theory and beyond: An Introduction to the Replica Method and Its Applications*, Vol. 9 (World Scientific Publishing Co Inc, 1987).
- [33] W. H. Nitsche, N. Y. Kim, G. Roumpos, C. Schneider, M. Kamp, S. Höfling, A. Forchel, and Y. Yamamoto, *Phys. Rev. B* **90**, 205430 (2014).